Caspian Journal of Environmental Sciences
Online ISSN: 1735-3866
Print ISSN: 1735-3033

Challenges in otolith shape analysis in riverine gobies: Effects of growth and asymmetry

Fatah Zarei[1]*, Hamid Reza Esmaeili[2]*, Tholoana Ntokoane[1], Reza Sadeghi[3]

[1.] *NRF-South African Institute for Aquatic Biodiversity, Private Bag 1015, Makhanda 6140, South Africa*
[2.] *Ichthyology and Molecular Systematics Research Laboratory, Zoology Section, Department of Biology, College of Sciences, Shiraz University, Shiraz, Iran*
[3.] *Department of Biology, Bo. C., Islamic Azad University, Borujerd, Iran*

**Corresponding authors' E-mail: Fatah Zarei (f.zarei@saiab.nrf.ac.za); Hamid Reza Esmaeili (hresmaeili@shirazu.ac.ir)*

ABSTRACT
Otolith morphology has long been a valuable tool in fish taxonomy and, more recently, in stock assessment and the analysis of intraspecific population structure. However, it is influenced by a complex interplay of intrinsic and extrinsic factors, which can introduce variability and obscure meaningful patterns. This study investigated the effects of two such factors, ontogenetic development and left-right asymmetry, on otolith shape in two south Caspian riverine gobiid species, *Ponticola gorlap* and *P. patimari*, using single-population samples while controlling for other variables. Results showed strong, consistent ontogenetic effects: smaller individuals exhibited compact shapes, whereas larger individuals had more elongate outlines with pronounced regional features. Left-right asymmetry was also evident, with inconsistent directional trends suggesting developmental noise rather than functional adaptation. Wavelet-based classification accuracy was modest (overall classification: 32.2% and 40.9%, respectively), reflecting considerable morphological overlap among size classes and emphasizing the limitations of relying solely on otolith shape for population discrimination. These findings highlight the need to standardise for growth, analyse both otoliths when feasible, and integrate otolith data with complementary sources such as molecular information. Such an integrative approach is essential for accurately interpreting otolith shape variation and ensuring effective management of fish populations.

Keywords: Sagittae, Intraspecific variation, Left-right asymmetry, Ontogenetic variation, Wavelet shape descriptors.

INTRODUCTION

In teleost fishes, the inner ear contains three pairs of otoliths, sagittae (saccular), lapilli (utricular), and asterisci (lagenar), which are aragonitic, biomineralised structures that develop independently of the skeletal system and are essential for auditory perception and balance (Campana 1999; Popper & Fay 2011; Schulz-Mirbach *et al*. 2019). Otolith analysis has become a key tool in ichthyological research, contributing significantly to our understanding of teleost systematics, phylogenetics, biogeography, population structure and stock assessment, climatic patterns, life history traits, and habitat use (e.g., Campana & Thorrold 2001; Andrus *et al*. 2002; Tuset *et al*. 2016; Zarei *et al*. 2023b). The sagittal otolith, hereafter referred to as the 'otolith', is typically the largest of the three and is of particular interest, especially to fish taxonomists and palaeontologists, due to its distinct and variable morphology, which reflects differences across species, genera, and higher taxonomic levels (e.g., Tuset *et al*. 2008; Sadeghi *et al*. 2020; Zarei *et al*. 2023b).

Caspian J. Environ. Sci.
DOI:
Received:
Article type: Research

Traditionally, otoliths have been used in systematic and paleontological studies through descriptive methods that focused on qualitative description of shape, size, and key structural features such as the morphology of the sulcus acusticus (e.g., Nolf 1985; Assis 2003). These observations were often complemented by morphometric approaches using linear measurements (e.g., otolith length, height, and width) and several derived shape indices (e.g., aspect ratio, circularity, rectangularity, and ellipticity) to quantify both interspecific and intraspecific variations (e.g., Tuset *et al*. 2008). Despite their foundational role, these early approaches were inherently subjective and insufficient for resolving the detailed morphological complexity of otoliths. Recent advances in computational morphometrics have significantly enhanced the accuracy and reproducibility of otolith-based analyses by minimizing observer bias and enabling high-resolution shape quantification (Lombarte *et al*. 2010). For instance, the development of the shapeR package in R has facilitated the automated extraction of otolith contours and the application of Elliptic Fourier and wavelet transforms to detect subtle morphological variations among closely related species and populations (Libungan & Pálsson 2015). These advancements have significantly enhanced the discriminatory power of otolith analysis in alpha taxonomy, stock assessment, and studies of intraspecific variation.

Otolith morphology is shaped by a complex interplay of intrinsic and extrinsic factors. Intrinsic determinants such as genetic architecture, ontogenetic stage, and sex significantly influence otolith shape. At the same time, external environmental factors such as temperature, salinity, depth, and water flow influence otolith formation by impacting both somatic growth patterns and the deposition of calcium carbonate. In addition, ecological factors such as migratory behavior and anthropogenic influences like pollutant exposure can induce physiological changes that are reflected in otolith shape, often revealing habitat-specific traits or indicators of environmental stress (e.g., Oozeki *et al*. 2000; Vignon & Morat 2010; Berg *et al*. 2018; Vignon 2018; Di Franco *et al*. 2019; Assis *et al*. 2020; Clark *et al*. 2021; Hong *et al*. 2021). These multidimensional influences pose challenges for otolith-based analyses in taxonomic and paleontological research, highlighting the importance of understanding them when applying otolith shape analysis.

The recent integration of otolith morphology with traditional morphological and molecular data in extant Ponto-Caspian gobies (Teleostei: Gobiidae) has both supported and challenged established taxonomic frameworks. Qualitative and quantitative analyses have underscored the diagnostic and phylogenetic relevance of otoliths at the tribal, generic, and species levels (Zarei *et al*. 2023b). However, studies on several riverine species have revealed marked intraspecific variation in otolith shape, which often shows limited correspondence with phylogenetic groupings or geographic patterns of genetic diversity (Zarei *et al*. 2022, 2023a). This discordance suggests that, while genetic factors may define the baseline otolith morphology of a species or lineage, shape can be strongly modulated by developmental, environmental, ecological, and anthropogenic influences. Additionally, a residual component of unexplained variation, likely arising from stochastic developmental processes, further complicates interpretation. These diverse sources of variability introduce noise into otolith shape analyses, potentially obscuring meaningful patterns. Acknowledging and addressing this complexity is crucial for improving the accuracy and interpretability of otolith-based taxonomic and population-level studies.

To address key methodological challenges in intraspecific otolith shape analysis, this study examined the effects of ontogenetic development and left-right otolith asymmetry on the outcomes of otolith shape analyses. We focused on two riverine gobiid species, *Ponticola gorlap* (Iljin, 1949) and *P. patimari* Eagderi, Nikmehr & Poorbagher 2020, collected during a 2023 field survey from 200-meter stretches of two rivers in the Southern Caspian Sea sub-basin, Northern Iran, thereby minimizing potential confounding temporal, geographic, phylogenetic, environmental, and anthropogenic influences. By systematically sampling across defined size classes and comparing left and right otoliths from the same individuals, we aimed to isolate and quantify the influence of intrinsic developmental processes. The findings provide critical insight into the reliability and limitations of otolith shape analysis for inferring intraspecific population structure in riverine gobiids, emphasizing the need for careful consideration of growth-related variation and asymmetry in studies of population structure and taxonomic resolution.

MATERIALS AND METHODS

Sampling

Specimens of *Ponticola gorlap* (n = 166) and *P. patimari* (n = 99) were collected on 10 and 11 June 2023 from 200-meter stretches of the Babol Roud (36°36′22.8″N, 52°38′35.1″E) and Shafa Roud (37°31′42.0″N,

Received:
Article type: Research

49°06′03.9″E) rivers, respectively, in the Southern Caspian Sea sub-basin, Northern Iran (Fig. 1). Fish were captured using hand nets and anesthetised with clove oil. Specimens were immediately preserved in 70% ethanol and subsequently archived in the first author's personal fish collection. Total length (TL) and standard length [SL: from the anteriormost point of the upper lip to the posterior end of the hypural plate (base of the caudal fin)] were measured to the nearest 0.1 mm using a digital caliper. Specimens were assigned to one of three size classes per species based on either TL or SL, with no overlap among size classes for either measurement (Table 1). To maintain balanced sex ratios across size groups, sex was determined in the field based on urogenital papilla morphology, and surplus individuals were released alive at the capture site. Therefore, each size class contained a similar number of males and females. It should be noted that potential differences in otolith shape between males and females of the Southern Caspian species of *Ponticola* (*P. gorlap*, *P. patimari*, and *P. iranicus*) have already been analysed using shapeR by Zarei *et al*. (2022, 2023a), and their results demonstrated no significant differences in otolith shape between sexes.

Table 1. Specimens and otolith materials used in this study.

Species	Size class	TL (mm)	SL (mm)	N	Sagittae	
					Left	Right
Ponticola gorlap	G1	52.8–77.2	41.7–60.9	52	G1_L	G1_R
	G2	78.1–93.0	62.9–75.2	66	G2_L	G2_R
	G3	93.2–118.9	75.6–95.75	48	G3_L	G3_R
Ponticola patimari	P1	39.2–54.6	32.9–43.0	35	P1_L	P1_R
	P2	55.8–70.7	44.0–54.9	35	P2_L	P2_R
	P3	72.1–95.9	55.3–75.6	29	P3_L	P3_R

Note: TL, total length; SL, standard length; N, number of specimens.

Otolith shape analysis

Left and right sagittal otoliths were extracted under a microscope using fine-tipped tweezers, cleaned by incubation in a 3% KOH solution, rinsed with distilled water, and air-dried at room temperature. Terminology for sagittae follows Gierl *et a*l. (2018) and Schwarzhans *et al*. (2020). The otoliths were placed on a dark background and imaged using an Olympus SZX10 stereomicroscope equipped with a digital camera at the Department of Biology, University of Sulaimani, Sulaymaniyah, Iraq. Images of the right otoliths were horizontally flipped to enable direct comparison with the left otoliths. Shape variation was analysed in R version 4.0.5 (Ihaka & Gentleman 1996) using statistical functions from the packages *shapeR* 0.1-5 (Libungan & Pálsson 2015), *vegan* 2.5-7 (Oksanen *et al*. 2020), *ipred* 0.9-12 (Peters *et al*. 2021), and *MASS* 7.3-54 (Ripley *et al*. 2021). JPEG images were imported into R, and coordinate matrices (x, y) were generated from all otolith outlines. Evenly spaced radii, measured by length as a univariate shape descriptor, were drawn from each otolith's centroid to its outline. Wavelet coefficients were extracted using *wavethresh* 4.6.8 (Nason 2016); coefficients exhibiting significant interaction between samples and total length were excluded from further analysis. Mean otolith shapes were then reconstructed and visualised based on the retained wavelet coefficients. To determine regions of shape variation, mean shape coefficients and their standard deviations were plotted against the angle of the outlines using wavelet transform with *gplots* 3.1.1 (Warnes *et al*. 2020). The radii length was used to test the significance of differences between samples based on ANOVA-like permutation tests in *vegan*. Standardised wavelet coefficients were transformed into principal coordinates and analysed using canonical analysis of principal coordinates (CAP). The resulting CAP scores were visualised along the first two discriminating axes (CAP1 and CAP2) to explore group clustering. These CAP results were then used to construct a dendrogram based on squared Euclidean dissimilarity in IBM SPSS version 26. Classification success was evaluated using a leave-one-out cross-validation approach. Linear Discriminant Analysis (LDA) was performed on the standardised wavelet coefficients to assess the accuracy of assigning individuals to their original groups. This analysis was implemented using the *errorest* function in *ipred* and the *lda* function in *MASS*.

RESULTS

General morphology of the sagittal otolith

Ponticola gorlap: The overall shape of the otolith is an elongated parallelogram (Fig. 1a), with an aspect ratio (otolith length/height) of 1.3–1.6. The dorsal rim (*dr*) is horizontal, irregularly sinuate, and dentate, with a slight

Received:
Article type: Research

anterior depression. The predorsal angle (*pda*) is obtuse. The posterodorsal projection (*pdp*) is moderately long, tapering, and either pointed or blunt at the tip, and is strongly bent outward. The anterior rim (*ar*) is oblique, with an inclination angle (β) of 66.1–81.3˚, and is either not incised or only slightly incised at or above the level of the ostium. The posterior rim (*pr*) runs nearly parallel to the anterior rim or is slightly less oblique, with an inclination angle (γ) of 92.5–104.6˚, and features a distinct concavity at or just above the level of the cauda. The inclination angle (δ) of the line connecting the preventral angle to the tip of the posterodorsal projection is 24–28˚. The ventral rim is horizontal, either entire or slightly undulate, and gently projects downward near the posterior end. The preventral projection is long and either pointed or blunt. The posteroventral angle is generally broadly rounded, and may be undulate, crenate, or denticulate. The sulcus is centrally positioned and sole-shaped, with moderate depth. The ostial lobes are well-developed, long, and relatively broad. The ostium has an inclination angle (α) of 9.4–18.8˚. The ratio of minimal otolith length to colliculum length is 1.4–1.5. A slender subcaudal iugum is present, approximately one-third the length of the cauda. The ventral furrow runs at a moderate to close distance from the ventral rim. The dorsal depression is distinct and ranges from narrow to moderately wide.

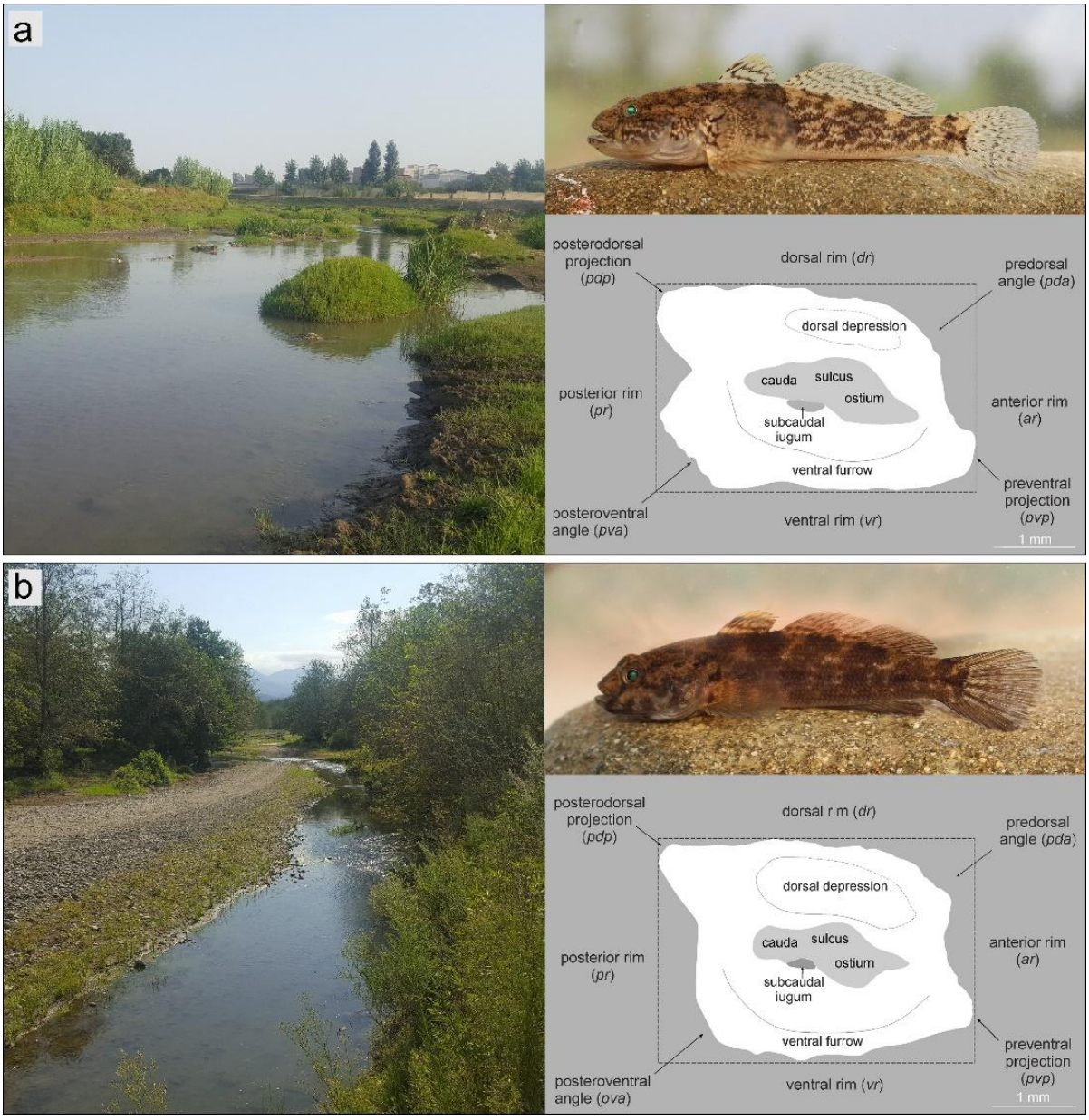

Fig. 1. Collection sites and sagittal otoliths of two gobiid species from the southern Caspian Sea sub-basin, Northern Iran. (a) *Ponticola gorlap* from the Babol Roud River; (b) *P. patimari* from the Shafa Roud River. Schematic drawings of the sagittal otoliths are based on Zarei *et al*. (2023b).

Caspian J. Environ. Sci.
DOI:

Received:
Article type: Research

Ponticola patimari: The otolith has an elongated parallelogram shape, with an aspect ratio (otolith length/height) of 1.4–1.6 (Fig. 1b). The dorsal rim (*dr*) is horizontal, entire, and either crenate or sinuate. The predorsal angle (*pda*) is orthogonal to slightly obtuse. The posterodorsal projection is long, strongly bent outward, and typically slightly upward-directed dorsally; its tip is usually pointed or blunt. The anterior rim is oblique, with an inclination angle (β) of 68.1–77.8˚, and may be either incised or unincised at the level of the ostium. The posterior rim runs nearly parallel to the anterior rim, with an inclination angle (γ) of 98.5–109.5˚, and presents either a smooth margin or a shallow concavity. The inclination angle (δ) of the line connecting the preventral angle to the tip of the posterodorsal projection is 22.2–27.6˚. The ventral rim is horizontal and usually entire to slightly undulate. The preventral projection is long and either pointed or blunt at the tip. The posteroventral angle is orthogonal and typically entire to slightly undulate. The sulcus is centrally positioned and sole-shaped, very deep, with well-developed ostial lobes. The inclination angle of the ostium (α) ranges from 7.8 to 13.8˚. The ratio of minimal otolith length to colliculum length is 1.5–1.8. A subcaudal iugum is usually absent or very small, slender, and measuring about one-half to one-third the length of the cauda. The ventral furrow runs at a moderate distance from the ventral rim. The dorsal depression is usually distinct and moderately wide.

Otolith shape analysis

Ponticola gorlap

Between-group comparisons. An ANOVA-like permutation test revealed that all between-group comparisons (i.e., G1 vs. G2. vs. G3) were statistically significant, except for Group 3 right otoliths (G3_R) versus Group 2 otoliths (G2_L and G2_R) (Table 2). Comparisons of mean otolith outlines, based on standardised wavelet coefficients, indicated significant differences among the three groups at several key regions: the preventral projection (*pvp*), anterior rim (*ar*), dorsal rim (*dr*), posterodorsal projection (*pdp*), posterior rim (*pr*) below the projection, and posterior half of ventral rim (*vr*) (Fig. 2a). Group 1 (TL: 52.8–77.2 mm) exhibited the innermost outline at the *pvp*, *ar*, *pdp*, and *pr* below the projection, and the outermost outline at the *dr* and posterior half of *vr*. In contrast, Group 3 (TL: 93.2–118.9 mm) showed the outermost outline at the *pvp*, *ar*, *pdp*, and *pr* below the projection, and the innermost outline at the *dr* and posterior half of *vr*. Group 2 (TL: 78.1–93.0 mm) displayed intermediate outlines across all these regions.

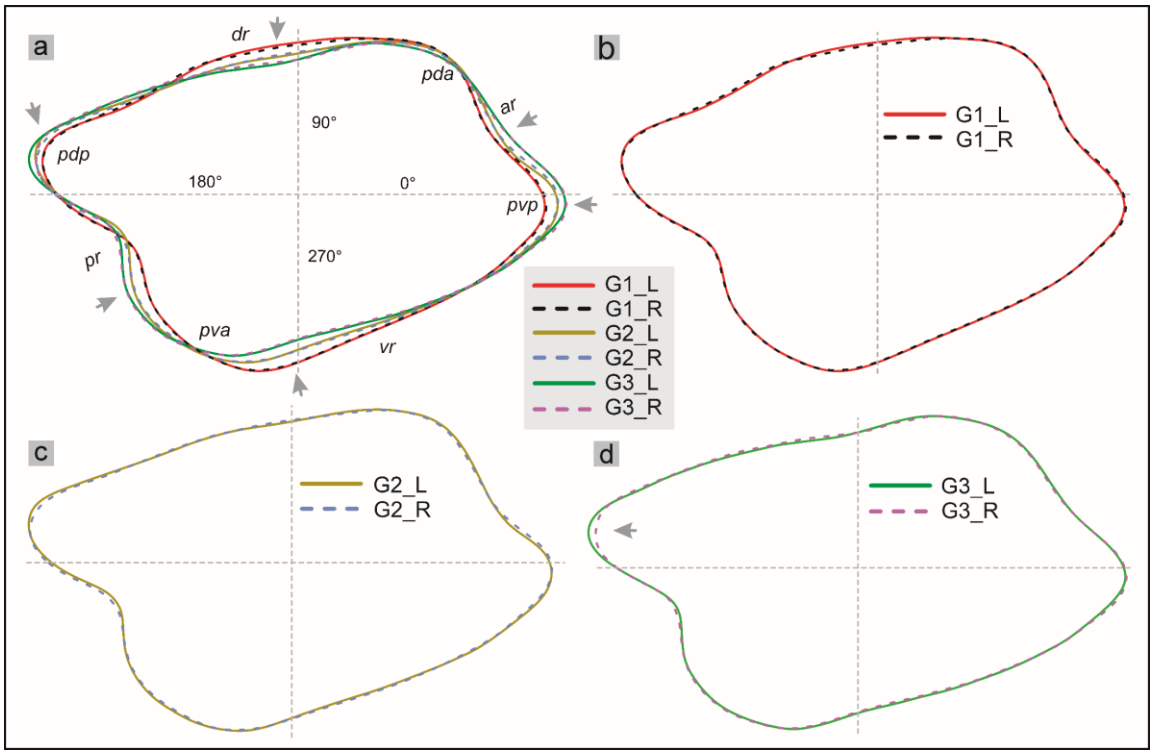

Fig. 2. Mean otolith shape comparisons in *Ponticola gorlap*. (a) Differences among the three size groups (G1, G2, G3); (b) left vs. right otoliths in Group 1; (c) left vs. right otoliths in Group 2; and (d) left vs. right otoliths in Group 3.

Caspian J. Environ. Sci.
DOI:
Received:
Article type: Research

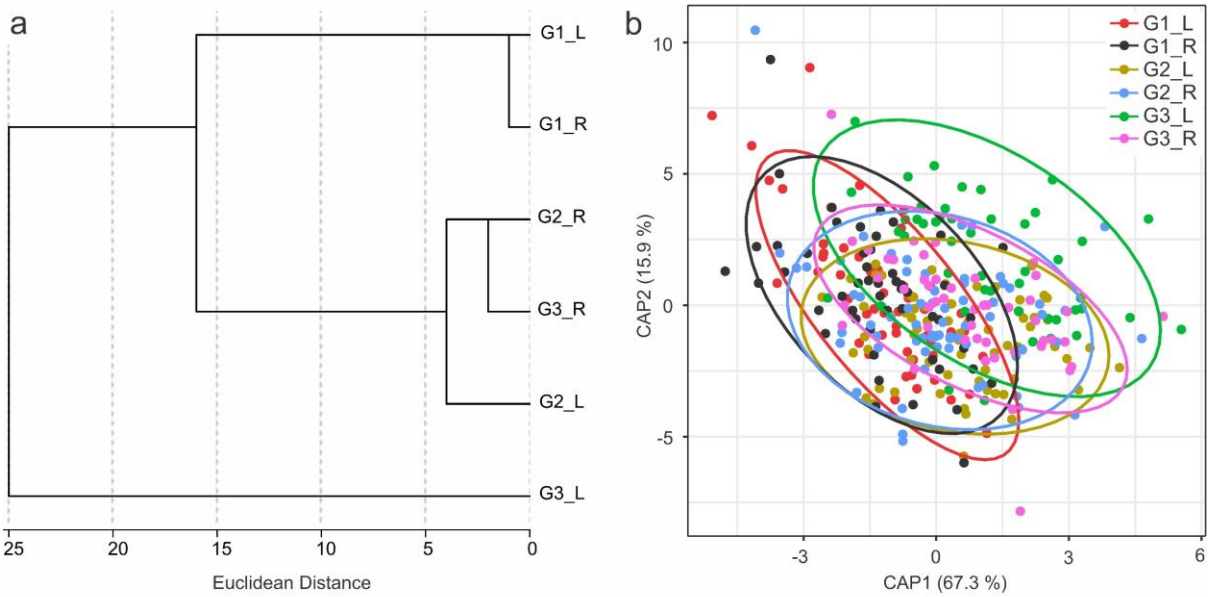

Fig. 3. (a) Hierarchical cluster analysis based on otolith shape data using Euclidean distance, illustrating phenotypic relationships among *Ponticola gorlap* samples. (b) Canonical scores for each *P. gorlap* sample plotted on the first two discriminating axes (CAP1 and CAP2), derived from wavelet-based analysis.

Within-group comparisons. An ANOVA-like permutation test based on otolith radii revealed no significant intra-group differences between the left and right sagittae in Group 1 (i.e., G1_L vs. G1_R) and Group 2 (i.e., G2_L vs. G2_R) (Table 2).

However, a significant difference was detected in Group 3 (i.e., G3_L vs. G3_R). Specifically, the left and right sagittae in Group 3 (i.e., G3_L and G3_R, respectively) differed significantly at the posterodorsal projection (*pdp*) (Fig. 2d). At this region, G3_R was more similar to both the left and right sagittae in Group 2 (i.e., G2_L and G2_R, respectively). Cluster analysis based on canonical analysis of principal coordinates (CAP) using Euclidean distances (Table S1) identified three distinct clusters (Fig. 3a): G3_L formed a separate cluster; G1_L and G1_R grouped together in a second cluster; and G2_L, G2_R, and G3_R formed a third cluster. The first two CAP axes, derived from standardised wavelet coefficients, explained 83.2% of the total variation among samples (CAP1 = 67.3%, CAP2 = 15.9%), illustrating the spatial distribution of the three clusters (Fig. 3b). The overall classification success, based on leave-one-out cross-validation, was 32.2%. The highest classification accuracy was observed for G3_L, with a success rate of 72.9% (Table 3).

Table 2. Results of the ANOVA-like permutation test comparing otolith shape between and within groups of *Ponticola gorlap*.

Comparison	df	SS	F-value	P-value
G1_L v. G2_L	1	4.054	7.0533	0.001
G1_L v. G3_L	1	6.228	10.005	0.001
G1_L v. G1_R	1	0.596	1.0776	**0.349**
G1_L v. G2_R	1	2.247	3.6813	0.002
G1_L v. G3_R	1	4.946	7.8985	0.001
G2_L v. G3_L	1	2.911	4.571	0.001
G2_L v. G1_R	1	4.738	8.2348	0.001
G2_L v. G2_R	1	0.744	1.1916	**0.270**
G2_L v. G3_R	1	1.860	2.9062	**0.053**
G3_L v. G1_R	1	6.91	11.09	0.001
G3_L v. G2_R	1	2.741	4.0682	0.001
G3_L v. G3_R	1	2.168	3.0866	0.001
G1_R v. G2_R	1	2.861	4.6824	0.001
G1_R v. G3_R	1	4.897	7.8124	0.001
G2_R v. G3_R	1	1.754	2.5911	**0.056**

Note: df, degrees of freedom; SS, sum of squares.

Caspian J. Environ. Sci.
DOI:

Received:
Article type: Research

Table 3. Classification results based on Linear Discriminant Analysis (LDA) of standardised wavelet coefficients for *Ponticola gorlap* samples. Overall classification (cross-validated): 32.2%.

	G1_L	G2_L	G3_L	G1_R	G2_R	G3_R
G1_L	**13.5**	30.8	5.8	42.3	3.8	3.8
G2_L	12.1	**28.8**	10.6	15.2	10.6	22.7
G3_L	4.2	4.2	**72.9**	4.2	0.0	14.6
G1_R	25.0	17.3	7.7	**42.3**	3.8	3.8
G2_R	10.6	33.3	16.7	16.7	**10.6**	12.1
G3_R	6.3	16.7	18.8	10.4	12.5	**35.4**

Ponticola patimari

Between-group comparisons. An ANOVA-like permutation test revealed that all between-group comparisons (i.e., P1 vs. P2. vs. P3) were significant (Table 4). Mean outline comparisons indicated that the three groups differed significantly at the *pvp*, *ar* above the concavity, *dr*, *pdp*, and posterior *vr* (Fig. 4a). Specifically, P1 (TL: 39.2–54.6 mm) exhibited the innermost outline at the *pvp* and *ar* above the concavity, and the outermost outline at the *dr* and posterior *vr*. P2 (TL: 55.8–70.7 mm) and P3 (TL: 72.1–95.9 mm) showed similar outlines, differing primarily at the mid-length of the *dr*, where P2 displayed the innermost and P3 the intermediate outline.

Within-group comparisons. The ANOVA-like permutation test based on radii revealed no significant intra-group differences between the left and right sagittae in Group 2 (P2_L vs. P2_R) and Group 3 (P3_L vs. P3_R). However, a significant difference was observed in Group 1 (P1_L vs. P1_R) (Table 4). Specifically, the left and right sagittae in Group 1 differed significantly in their *pdp* (Fig. 4b). Cluster analysis based on CAP1 and CAP2 using Euclidean distance (Table S2) identified four main clusters (Fig. 5a): one for P1_R, one for P1_L, one comprising P2_L and P2_R, and another comprising P3_L and P3_R. The first two canonical axes explained 74.5% of the variation among samples (CAP1 = 46.6%, CAP2 = 27.9%) (Fig. 5b). Overall classification success, based on a leave-one-out cross-validation, was 40.9%, with the highest accuracy achieved for P1_R (71.4%) and P1_L (65.7%) (Table 5).

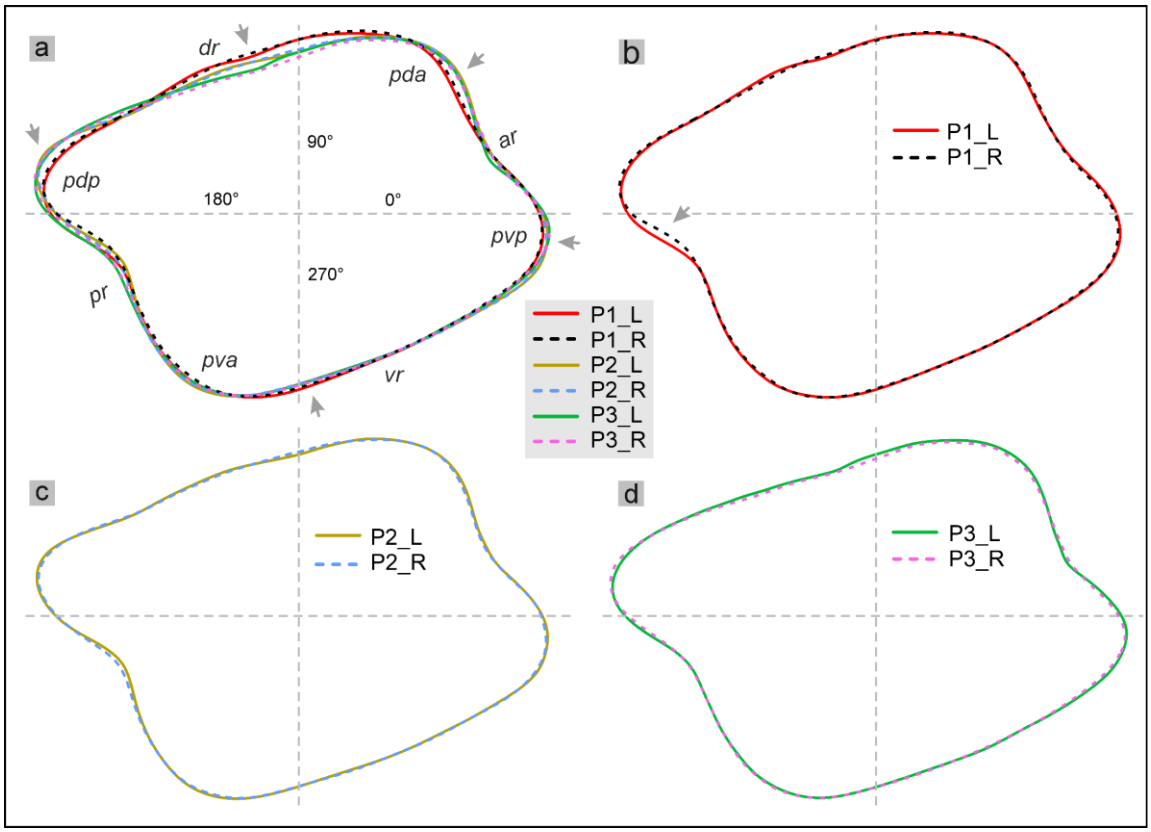

Fig. 4. Mean otolith shape comparisons in *Ponticola patimari*. (a) Differences among the three size groups (P1, P2, P3); (b) left vs. right otoliths in Group 1; (c) left vs. right otoliths in Group 2; and (d) left vs. right otoliths in Group 3.

Caspian J. Environ. Sci.
DOI:

Received:
Article type: Research

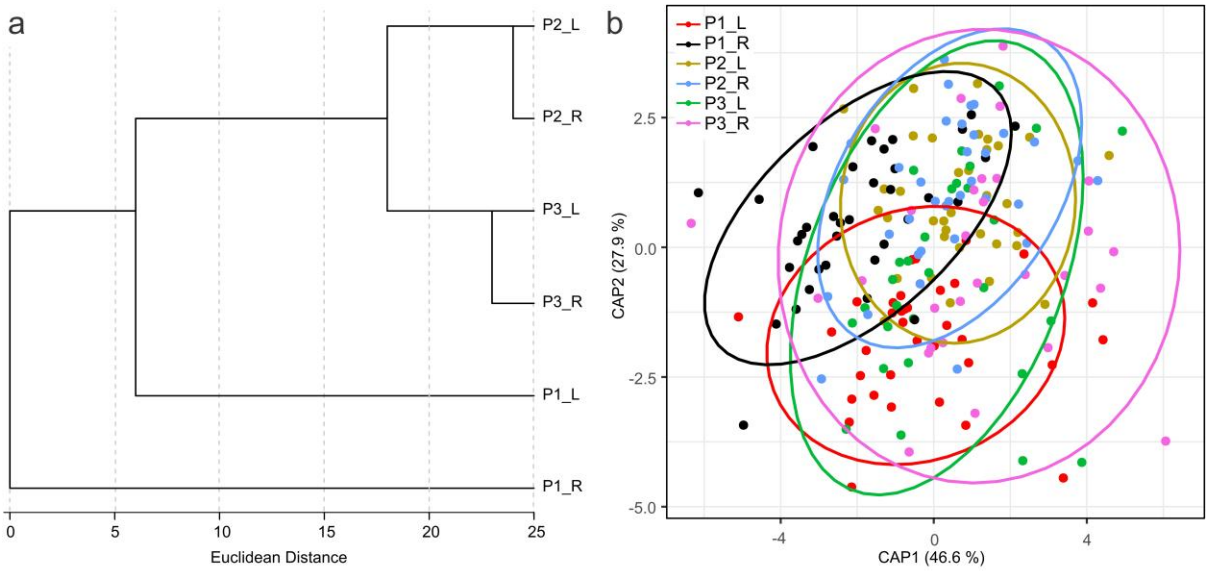

Fig. 5. (a) Hierarchical cluster analysis based on otolith shape data using Euclidean distance, illustrating phenotypic relationships among *Ponticola patimari* samples. (b) Canonical scores for each *P. patimari* sample plotted on the first two discriminating axes (CAP1 and CAP2), derived from wavelet-based analysis.

Table 4. Results of the ANOVA-like permutation test comparing otolith shape between and within groups of *Ponticola patimari*.

Comparison	df	SS	F-value	P-value
P1_L v. P2_L	1	3.388	4.183	0.006
P1_L v. P3_L	1	2.282	2.1407	0.008
P1_L v. P1_R	1	4.790	5.8827	0.001
P1_L v. P2_R	1	3.477	4.1005	0.007
P1_L v. P3_R	1	3.759	3.3408	0.004
P2_L v. P3_L	1	1.99	2.0336	0.041
P2_L v. P1_R	1	5.161	7.0237	0.001
P2_L v. P2_R	1	0.169	0.2197	**0.996**
P2_L v. P3_R	1	2.238	2.1566	0.042
P3_L v. P1_R	1	4.238	4.3089	0.001
P3_L v. P2_R	1	1.844	1.8076	0.044
P3_L v. P3_R	1	1.178	0.875	**0.524**
P1_R v. P2_R	1	4.189	5.421	0.001
P1_R v. P3_R	1	6.069	5.8201	0.001
P2_R v. P3_R	1	2.265	2.0983	0.043

Note: df, degrees of freedom; SS, sum of squares.

Table 5. Classification results based on Linear Discriminant Analysis (LDA) of standardised wavelet coefficients for *Ponticola patimari* samples. Overall classification (cross-validated): 40.9%.

	P1_L	P2_L	P3_L	P1_R	P2_R	P3_R
P1_L	**65.7**	0.0	14.3	5.7	0.0	14.3
P2_L	2.9	**20.0**	8.6	14.3	31.4	22.9
P3_L	41.4	10.3	**13.8**	0.0	24.1	10.3
P1_R	8.6	8.6	0.0	**71.4**	11.4	0.0
P2_R	8.6	20.0	8.6	14.3	**37.1**	11.4
P3_R	24.1	13.8	3.4	13.8	13.8	**31.0**

DISCUSSION

Otolith morphology has long been a cornerstone in fish taxonomy, providing key diagnostic traits across a wide range of taxonomic levels. In recent years, otolith shape analysis has also emerged as a valuable method for assessing population structure and stock differentiation at the intraspecific level (e.g., Vieira *et al*. 2014; Jemaa *et al*. 2015; Moreira *et al*. 2019; Sadeghi *et al*. 2020). However, compared with molecular data, otolith shape is influenced by a range of intrinsic and environmental factors, making the interpretation of intraspecific

Received:
Article type: Research

morphological variation complex and potentially compromising the reliability of analytical outcomes. Our previous studies of the Caspian gobies confirm this complexity (Zarei *et al.* 2022, 2023a,b). Zarei *et al*. (2023b) demonstrated taxonomic differentiation in otolith morphology across species, genera, and tribes of the Caspian gobies, including the riverine species of the genus *Ponticola* in the South Caspian sub-basin. *Ponticola gorlap* differed from *P. iranicus* and *P. patimari* in five and four otolith variables, respectively. Despite these differences, species-level classification success was only 60% for *P. gorlap*, 50% for *P. iranicus*, and 40% for *P. patimari*, indicating considerable morphological overlap among these species. In a study of the population structure of *P. gorlap* across the South Caspian sub-basin based on mitochondrial DNA control-region sequences and otolith shape, Zarei *et al.* (2023a) found significant otolith-shape differences among all seven sampled populations (Chalvand, Siahdarvishan, Sefidroud, Polroud, Babolroud, Nekaroud, and Kaboudval). However, overall cross-validated classification success among these populations based on otolith shape was only 30.9%, and the pattern of otolith-shape variation did not correspond closely to the distribution of genetic variation. Zarei *et al*. (2022) similarly investigated the population structure of *P. patimari* and *P. iranicus* in the Southern Caspian rivers (Karganroud, Shafaroud, Siahdarvishan, Sefidroud, Polroud, Tonekabon, Chalus, Nowshahr, and Kheirud) using otolith shape and mitochondrial COI data. They obtained only 43.7% overall cross-validated classification success based on otolith shape and again found that the observed morphological pattern did not correspond to the phylogeographic pattern revealed by the molecular data. Thus, our previous studies demonstrated both the taxonomic utility of otolith shape and substantial morphological overlap and variation at the species and intraspecific levels, but did not establish the extent to which this variation might be attributable to ontogenetic development or bilateral otolith asymmetry. In this study, we examined the influence of ontogenetic development and left-right otolith asymmetry on shape analysis results in *P. gorlap* and *P. patimari*. By controlling for external variables and sampling a single population per species, we isolated these intrinsic factors to evaluate their potential confounding effects.

Our results show that ontogenetic change has a strong and consistent effect on otolith shape across both species, *P. gorlap* and *P. patimari*. Significant differences among size groups were concentrated in several regions of the otolith outline, particularly in the preventral projection (*pvp*), anterior rim (*ar*), dorsal rim (*dr*), posterodorsal projection (*pdp*), posterior rim (*pr*) below the projection, and posterior half of ventral rim (*vr*). In both species, smaller individuals (G1, P1) had more compact otoliths with less pronounced anterior and posterior features, whereas larger individuals (G3, P3) had more elongate outlines and more developed projections. These findings emphasise that shape-based comparisons between individuals of different sizes can yield misleading interpretations if growth is not adequately accounted for. This is relevant to our previous population-level studies on both species because the populations analysed in Zarei *et al.* (2022, 2023a) included both small and large individuals within broad standard-length ranges, suggesting that population-level comparisons in those studies incorporated a component of ontogenetic variation. Given the pronounced size-related changes observed here, differences in the relative representation of size classes among populations could have contributed to the observed otolith-shape differences or obscured patterns more closely associated with population genetic structure. Therefore, the present results provide a plausible explanation for at least part of the discrepancy between otolith-shape and molecular patterns reported in Zarei *et al.* (2022, 2023a). A similar pattern was observed in our studies of *Istigobius ornatus* (Rüppell, 1830) from the Iranian coastal waters of the Persian Gulf and Gulf of Oman (Sadeghi *et al*. 2020, 2021), where otolith-shape variation did not closely correspond to the phylogeographic pattern inferred from molecular data. The use of specimens spanning broad size ranges within populations, including the Qeshm (South Iran) population, may have contributed to this discrepancy. These observations highlight the importance of controlling for size structure when using otolith shape to assess population differentiation or to compare morphological patterns with molecular population structure.

Variation in otolith shape between left and right sides was evident in larger individuals of *Ponticola gorlap* (G3_L vs. G3_R) and smaller individuals of *P. patimari* (P1_L vs. P1_R), particularly in the posterodorsal projection (*pdp*). This indicates that asymmetry is a common feature of otolith development and may affect shape-based analyses across both juvenile and adult stages. Notably, the direction of asymmetry was inconsistent, lacking any clear left- or right-side dominance, which suggests that the observed variation is stochastic in nature, likely arising from developmental noise rather than biologically or environmentally driven processes. In addition, classification accuracy based on wavelet-derived shape descriptors was generally low, with overall success rates of 32.2% in *P. gorlap* and 40.9% in *P. patimari*, indicating considerable overlap in otolith morphology among size classes.

Received:
Article type: Research

Although some size-specific clusters (e.g., G3_L in *P. gorlap* and P1_L/R in *P. patimari*) exhibited clearer separation, the overall cross-validated performance underscores the limitations of relying solely on otolith outline data to uncover intraspecific population structure.

The observed effects of both ontogeny and bilateral variation demonstrated here within single populations of *P. gorlap* and *P. patimari* have important methodological implications for intraspecific population structure analyses. First, otolith shape should be regarded as complementary rather than primary evidence for assessing population structure in riverine gobiids across their geographic range. Molecular phylogeographic data provide a more appropriate primary framework for assessing population structure, while otolith morphology can provide complementary phenotypic evidence when interpreted alongside genetic data. This distinction is particularly important for the South Caspian riverine gobiids, where our previous studies (Zarei *et al*. 2022, 2023a) have shown that patterns of otolith-shape differentiation do not correspond to molecular phylogeographic structure. Second, population-level analyses of otolith shape should use comparable size classes across all study populations, ideally adults or clearly defined ontogenetic groups, to minimise variation associated with growth. Finally, the otolith side (i.e., left or right otolith) should also be standardised across all populations, as bilateral differences may contribute to variation and bias comparisons.

Finally, the ontogenetic differences observed in both species, particularly in the *pvp*, *ar*, *dr*, *pdp*, *pr*, and posterior *vr*, indicate that otolith growth is not proportional across the outline. Smaller individuals had more compact otoliths with less-developed projections, whereas these features became progressively more pronounced in larger individuals. The close similarity in this pattern of shape change from G1/P1 to G3/P3 in both species suggests that it represents a common intrinsic feature of otolith development, likely resulting from differential growth of individual regions of the otolith during ontogeny (Lombarte & Lleonart 1993). Since each species was sampled from a single 200-m river stretch during the same field survey, environmental variation was minimised by design, making an ecological explanation for the parallel size-related pattern less likely.

ACKNOWLEDGMENTS

This research was partly financially supported by Shiraz University, which is gratefully acknowledged. The subsequent continuation and completion of this research by FZ following the field sampling were supported by an NRF-South African Institute for Aquatic Biodiversity postdoctoral fellowship. The authors acknowledge that opinions, findings and conclusions or recommendations expressed in this publication, are those of the authors, and that the NRF accepts no liability whatsoever in this regard. We thank the two anonymous reviewers for their constructive and helpful comments, which have improved the manuscript.

CONFLICT OF INTEREST

There is no conflict of interest.

REFERENCES

Andrus, CFT, Crowe, DE & Romanek, CS 2002, Oxygen isotope record of the 1997–1998 El Nino in Peruvian sea catfish (*Galeichthys peruvianus*) otoliths. *Paleoceanography*, 17: 1053. https://doi.org/10.1029/2001PA000652

Assis, CA 2003, The utricular otoliths of teleosts: Their morphology and relevance for species identification and systematics studies. *Scientia Marina*, 67: 245–256. https://doi.org/10.3989/scimar.2005.69n2259

Assis, IO, da Silva, VE, Souto-Vieira, D, Lozano, AP, Volpedo, AV & Fabré, NN 2020, Ecomorphological patterns in otoliths of tropical fishes: Assessing trophic groups and depth strata preference by shape. *Environmental Biology of Fishes*, 103: 349–361. https://doi.org/10.1007/s10641-020-00961-0

Berg, F, Almeland, OW, Skadal, J, Slotte, A, Andersson, L & Folkvord, A 2018, Genetic factors have a major effect on growth, number of vertebrae and otolith shape in Atlantic herring (*Clupea harengus*). *PLoS ONE*, 13: e0190995. https://doi.org/10.1371/journal.pone.0190995

Campana, SE & Thorrold, SR 2001, Otoliths, increments, and elements: Keys to a comprehensive understanding of fish populations? *Canadian Journal of Fisheries and Aquatic Sciences*, 58: 30–38. https://doi.org/10.1139/f00-177

Received:
Article type: Research

Campana, SE 1999, Chemistry and composition of fish otoliths: Pathways, mechanisms and applications. *Marine Ecology Progress Series*, 188: 263–297, https://doi.org/10.3354/meps188263

Clark, FJK, da Silva Lima, CS & Pessanha, ALM 2021, Otolith shape analysis of the Brazilian silverside in two northeastern Brazilian estuaries with distinct salinity ranges. *Fisheries Research*, 243: 106094, https://doi.org/10.1016/j.fishres.2021.106094

Di Franco, A, Calò, A, Sdiri, K, Cattano, C, Milazzo, M & Guidetti, P 2019, Ocean acidification affects somatic and otolith growth relationship in fish: Evidence from an *in situ* study. *Biology Letters*, 15: 20180662. https://doi.org/10.1098/rsbl.2018.0662

Hong, P, Jiang, S & Katayama, S 2021, Experimental study on the influence of water temperature on the otolith formation of the marbled flounder (*Pseudopleuronectes yokohamae*). *International Aquatic Research*, 13: 119–128, https://doi.org/10.22034/iar.2021.1916978.1119

Jemaa, S, Bacha, M, Khalaf, G, Dessailly, D, Rabhi, K & Amara, R 2015, What can otolith shape analysis tell us about population structure of the European sardine, *Sardina pilchardus*, from Atlantic and Mediterranean waters? *Journal of Sea Research*, 96: 11–17. https://doi.org/10.1016/j.seares.2014.11.002

Libungan, LA & Pálsson, S 2015, ShapeR: An R package to study otolith shape variation among fish populations. *PLoS ONE*, 10: e0121102. https://doi.org/10.1371/journal.pone.0121102

Lombarte, A, Chic, Ò, Parisi-Baradad, V, Olivella, R, Piera, J & García-Ladona, E 2010, A web-based environment for shape analysis of fish otoliths. The AFORO database. *Scientia Marina*, 74: 239–242. https://doi.org/10.3989/scimar.2006.70n1147

Lombarte, A & Lleonart, J 1993, Otolith size changes related with body growth, habitat depth and temperature. *Environmental Biology of Fishes*, 37: 297–306, https://doi.org/10.1007/BF00004637

Moreira, C, Froufe, E, Vaz-Pires, P & Correia, AT 2019, Otolith shape analysis as a tool to infer the population structure of the blue jack mackerel, *Trachurus picturatus*, in the NE Atlantic. *Fisheries Research*, 209: 40–48, https://doi.org/10.1016/j.fishres.2018.09.010

Nason, G 2016, Package 'wavethresh': Wavelets statistics and transforms. CRAN

Nolf, D 1985, Otolithi Piscium. In: H-P Schultze (ed), Handbook of Paleoichthyology, Vol 10. Gustav Fischer Verlag, Stuttgart.

Oksanen, J, Blanchet, FG, Friendly, M, Kindt, R, Legendre, P & McGlinn, D 2020, Package 'vegan': community ecology package. CRAN

Oozeki, Y & Watanabe, Y 2000, Comparison of somatic growth and otolith increment growth in laboratory-reared larvae of Pacific saury, *Cololabis saira*, under different temperature conditions. *Marine Biology*, 136: 349–359, https://doi.org/10.1007/s002270050693

Peters, A, Hothorn, T, Ripley, BD, Therneau, T & Atkinson, B 2021, Package 'ipred': improved predictors. CRAN

Popper, AN & Fay, RR 2011, Rethinking sound detection by fishes. *Hearing Research*, 273: 25–36, https://doi.org/10.1016/j.heares.2009.12.023

Ripley, B, Venables, B, Bates, DM, Hornik, K, Gebhardt, A & Firth, D 2021, Package 'MASS': functions and datasets to support Venables and Ripley. ''Modern Applied Statistics with S''. CRAN

Sadeghi, R, Esmaeili, HR, Zarei, F & Reichenbacher, B 2020, Population structure of the ornate goby, *Istigobius ornatus* (Teleostei: Gobiidae), in the Persian Gulf and Oman Sea as determined by otolith shape variation using ShapeR. *Environmental Biology of Fishes*, 103: 1217–1230, https://doi.org/10.1007/s10641-020-01015-1

Sadeghi, R, Esmaeili, HR, Zarei, F & Reichenbacher, B 2021, Matrilineal evidence for genetic structure and Late Pleistocene demographic expansion of the Ornate goby *Istigobius ornatus* (Teleostei: Gobiidae) in the Persian Gulf and Oman Sea. *Marine Ecology*, 42: e12629. https://doi.org/10.1111/maec.12629

Schulz-Mirbach, T, Ladich, F, Plath, M & Heß, M 2019, Enigmatic ear stones: what we know about the functional role and evolution of fish otoliths. *Biological Reviews*, 94: 457–482, https://doi.org/10.1111/brv.12463

Schwarzhans, W, Agiadi, K & Carnevale, G 2020, Late Miocene-Early Pliocene evolution of Mediterranean gobies and their environmental and biogeographic significance. *Rivista Italiana di Paleontologia e Stratigrafia*, 126: 657–723, https://doi.org/10.13130/2039-4942/14185

Tuset, VM, Farré, M, Otero-Ferrer, JL, Vilar, A, Morales-Nin, B & Lombarte, A 2016, Testing otolith morphology for measuring marine fish biodiversity. *Marine and Freshwater Research*, 67: 1037–1048, https://doi.org/10.1071/MF15052

Caspian J. Environ. Sci.
DOI:

Received:
Article type: Research

Tuset, VM, Lombarte, A & Assis, CA 2008, Otolith atlas for the western Mediterranean, north and central eastern Atlantic. *Scientia Marina*, 72: 7–198, https://doi.org/10.3989/scimar.2008.72s17

Vieira, AR, Neves, A, Sequeira, V, Paiva, RB & Gordo, LS 2014, Otolith shape analysis as a tool for stock discrimination of forkbeard (*Phycis phycis*) in the Northeast Atlantic. *Hydrobiologia*, 728: 103–110. https://doi.org/10.1007/s10750-014-1809-5

Vignon, M & Morat, F 2010, Environmental and genetic determinant of otolith shape revealed by a non-parametric approach in the convict surgeonfish (*Acanthurus triostegus*). *Journal of Fish Biology*, 76: 784–794, https://doi.org/10.3354/meps08651

Vignon, M 2018, Short-term stress for long-lasting otolith morphology—brief embryological stress disturbance can reorient otolith ontogenetic trajectory. *Canadian Journal of Fisheries and Aquatic Sciences*, 75: 1713–1722, https://doi.org/10.1139/cjfas-2017-0110

Warnes, G, Bolker, B, Bonebakker, L, Gentleman, R & Huber, W 2020, Package 'gplots': various R programming tools for plotting data. CRAN

Zarei, F, Esmaeili, HR, Sadeghi, R, Reichenbacher, B, Schliewen, UK, Abbasi, K & Gholamhosseini, A 2023a, Phylogeography and population structure of *Ponticola gorlap* (Teleostei: Gobiidae) in an evolutionary distinctive and ecologically threatened Caspian Sea sub-basin. *Aquatic Sciences*, 85: 15, https://doi.org/10.1007/s00027-022-00913-z

Zarei, F, Esmaeili, HR, Sadeghi, R, Schliewen, UK, Kovačić, M, Abbasi, K & Gholamhosseini, A 2022, An integrative insight into the diversity, distribution, and biogeography of the freshwater endemic clade of *the Ponticola syrman* group (Teleostei: Gobiidae) in the Caucasus biodiversity hotspot. *Ecology and Evolution*, 12: e9300. https://doi.org/10.1002/ece3.9300

Zarei, F, Esmaeili, HR, Stepien, CA, Kovačić, M & Abbasi, K 2023b, Otoliths of Caspian gobies (Teleostei: Gobiidae): Morphological diversity and phylogenetic implications. *PLoS ONE*, 18: e0285857, https://doi.org/10.1371/journal.pone.0285857

Supplementary tables

Table S1. Dissimilarity matrix of average Euclidean distances for *Ponticola grorlap* based on otolith shape.

	G1_L	G2_L	G3_L	G1_R	G2_R	G3_R
G1_L	0.00					
G2_L	5.23	0.00				
G3_L	7.41	9.18	0.00			
G1_R	0.02	5.89	7.72	0.00		
G2_R	2.18	0.82	5.72	2.61	0.00	
G3_R	4.08	1.28	3.62	4.63	0.56	0.00

Table S2. Dissimilarity matrix of average Euclidean distances for *Ponticola patimari* based on otolith shape.

	P1_L	P2_L	P3_L	P1_R	P2_R	P3_R
P1_L	0.00					
P2_L	8.03	0.00				
P3_L	2.04	2.11	0.00			
P1_R	8.41	6.96	6.95	0.00		
P2_R	8.42	0.09	2.49	5.79	0.00	
P3_R	4.41	1.36	0.57	9.91	1.99	0.00

Caspian J. Environ. Sci.
DOI:

Received:
Article type: Research